Communication in Physical Sciences, 2024, 12(3): 1070-1080

Isolation and Characterizations of a Pentacyclic Glycoside from Methanolic Fraction of *Allium sativum* (Purple Garlic) Bulbs

Chinwendu Olive Ozoeze, Okenwa Uchenna Igwe and Johnbull Onyekachi Echeme
Received: 11 December 2024/Accepted: 05 March 2025/Published: 14 March 2025
https://dx.doi.org/10.4314/cps.v12i3.28

Abstract: *This study reports the isolation and structural elucidation of a novel pentacyclic glycoside from the methanolic extract of air-dried cloves of* Allium sativum *(purple garlic), a medicinal plant extensively utilized in traditional medicine for the management of inflammation, gastrointestinal disturbances, respiratory tract infections, asthma, hay fever, and related ailments. The compound, identified as a derivative of a pentacyclic triterpenoid, bears the IUPAC name* (2R,3R,4R,5R,6R)-6'-(hydroxymethyl)-1-methyl-(20-(tert-pentyl)-19-(m-tolyl)-7,8,9,10,11,12,13,14,15, 16, 17, 18, 19, 20, 21, 22-hexadecahydropicenyl) oxy)tetrahydro-2H-pyran-2,3,4-triol. *Its isolation was achieved through chromatographic techniques, and its structural features were characterized using a comprehensive suite of spectroscopic methods, including FTIR, ^1H and ^13C NMR, HSQC, and LC-MS. Spectral data revealed characteristic signals for methine, hydroxymethine, glycosidic, aromatic, and aliphatic functional groups, with HSQC establishing clear carbon-proton connectivity. FTIR analysis confirmed the presence of hydroxyl, ether, and aromatic functionalities, while mass spectrometry indicated a molecular ion peak consistent with the molecular formula* $C_{32}H_{54}O_7$ *and a molecular weight of 546.5 g/mol. This is the first report of the isolation of this glycosylated oleanane derivative from* Allium sativum, *further enriching the phytochemical knowledge of the plant and supporting its traditional therapeutic applications.*

Keywords: *Medicinal plant; Allium sativum; chromatography; isolation; spectroscopy*

Chinwendu Olive Ozoeze*
Department of Chemistry, Michael Okpara University of Agriculture Umudike,
P.M.B. 7267, Umuahia, Abia State, Nigeria
Email: chinwenduolive@gmail.com
Orcid id: 0009-0000-1011-6734

Okenwa Uchenna Igwe
Department of Chemistry, Michael Okpara University of Agriculture Umudike,
P.M.B. 7267, Umuahia, Abia State, Nigeria
Email: igwe.okenwa@mouau.edu.ng
Orcid id: 0009-0000-3361-5923

Johnbull Onyekachi Echeme
Department of Chemistry, Michael Okpara University of Agriculture Umudike,
P.M.B. 7267, Umuahia, Abia State, Nigeria
Email:

1.0 Introduction

Garlic (*Allium sativum*), a bulbous flowering plant in the family Amaryllidaceae, is widely cultivated and consumed globally for its culinary and medicinal properties. Originating from Central Asia and northeastern Iran, garlic has a rich history of use in traditional medicine across diverse cultures, including those of Egypt, Greece, China, and India (Block, 2010; Mahady *et al*., 2001). Its pungent bulbs, consisting of multiple cloves, are known to possess a broad spectrum of bioactive compounds that contribute to its reputed therapeutic properties.

For over 3,000 years, garlic has been used in the treatment of various ailments such as earaches, gastrointestinal disorders, respiratory infections, and parasitic infestations (Hahn, 1996). Scientific studies have reported that garlic exhibits diaphoretic, anti-inflammatory, bacteriostatic, antiviral, antioxidant, hypotensive, and anticancer activities (Newall *et al*., 1996; Lee *et al*., 2012; Kimura *et al*., 2017). Several of these effects are attributed to its diverse phytochemical composition, including sulfur-containing compounds, saponins, flavonoids, and glycosides (Morihara *et al*., 2017).

Despite the extensive phytochemical investigations conducted on *Allium sativum*, particularly focusing on its volatile sulfur

compounds, there remains a significant gap in the identification and structural elucidation of high-molecular-weight non-sulfur secondary metabolites, such as glycosides. These compounds may possess potent pharmacological properties that are yet to be fully understood or utilized. Pentacyclic triterpenoid glycosides, in particular, have shown promise in anti-inflammatory, anticancer, and antiviral therapies but have rarely been reported in garlic extracts.

The aim of this study is to isolate and characterise a novel pentacyclic glycoside from the methanolic fraction of air-dried cloves of *Allium sativum* (purple garlic), using advanced chromatographic and spectroscopic techniques. The structural identification is supported by FT-IR, 1H NMR, 13C NMR, 2D NMR, and LC-MS data, along with comparisons to existing literature values.

This research is significant in that it presents the first report of this specific pentacyclic glycoside from *Allium sativum*, contributing to the growing body of knowledge on garlic phytochemistry and potentially expanding the pharmacological applications of garlic-derived compounds in modern drug discovery and development.

2.0 Materials and Methods

2.1 Plant Material Collection and Identification

Fresh bulbs of purple garlic (*Allium sativum*) were purchased from Ogbete Main Market in Enugu, Enugu State, Nigeria. The plant materials were identified and authenticated by Mr. Ndukwe Ibe, a taxonomist in the Department of Forestry, Michael Okpara University of Agriculture, Umudike, Abia State, Nigeria.

2.2 Sample Preparation and Extraction

The outer scales of the garlic bulbs were removed, and the bulbs were separated into individual cloves. These cloves were washed thoroughly, chopped into smaller pieces, and air-dried in a well-ventilated room for five (5) months to ensure complete moisture removal.

The dried garlic cloves were pulverized using a Thomas Wiley milling machine and stored in airtight containers. Cold maceration was employed for extraction. One kilogram (1 kg) of the pulverized sample was percolated with seven (7) litres of 95% methanol in a glass jar and kept undisturbed for four (4) days to avoid frothing, following the method of John Bull & Afolabi (2011). The extract was filtered using Whatman No. 1 filter paper, and the filtrate was concentrated under reduced pressure using a digital Heidolph Rotary Evaporator (4000 series). The concentrated extract was further evaporated to dryness to obtain a crude extract.

2.3 Isolation and Purification of Bioactive Compound

The isolation procedure was adapted from previously reported methods by Johnbull and Afolabi (2011), Igwe and Echeme (2013), and Kwekowe *et al*. (2021), with slight modifications. A portion (5.2 g) of the crude extract was subjected to column chromatography using 600 g of silica gel (70–230 mesh, 600 mL column volume). The column was allowed to stand for 45 minutes before elution to eliminate air bubbles.

Sequential elution was carried out as follows:

Step 1: Elution with 100% petroleum ether (non-polar solvent), collecting 50 cm^3 fractions at a flow rate of 14 drops per minute.

Step 2: Elution with graded mixtures of petroleum ether and chloroform in the following ratios: 95:5, 90:10, 85:15, 80:20, 75:25, 70:30, 65:35, 60:40, 55:45, 40:60, 35:65, 30:70, 25:75, 20:80, 15:85, 10:90, and 5:95.

Step 3: Elution with mixtures of chloroform and ethyl acetate in similar graded ratios as above.

Step 4: Elution with mixtures of ethyl acetate and methanol in the same graded series.

Step 5: Final elution with 100% methanol (polar solvent).

This chromatographic procedure lasted six (6) days, yielding 118 fractions (PG1–PG118).

Further purification was achieved through Thin Layer Chromatography (TLC) using pre-coated TLC plates as the stationary phase and a suitable solvent system comprising petroleum ether, chloroform, ethyl acetate, and methanol as the mobile phase.

Fractions with similar Rf values were pooled together. A pure fraction designated PG18 (renamed PG1) appeared as a single yellowish spot on the TLC plate with an Rf value of 0.77.

Detection was done using iodine vapour in an iodine chamber.

2.4 Spectroscopic Characterization of Isolated Compound

2.4.1 FT-IR Analysis

Fourier Transform Infrared Spectroscopy (FT-IR) was used to identify functional groups present in the isolated compound PG1. The sample was analyzed using a Bruker INVENIO R FT-IR spectrometer in the transmission mode over a spectral range of 4000–400 cm^{-1}. A diamond crystal of ATR (Attenuated Total Reflectance) was used as the sample interface. The resulting spectrum was analyzed to identify characteristic functional groups, following the approach described by Schrader (1995).

2.4.2 NMR Spectroscopy

The isolated compound PG1 was analyzed using Nuclear Magnetic Resonance (NMR) spectroscopy on a 500 MHz Bruker AVANCE spectrometer. The spectra were acquired using deuterated solvents, specifically deuterated chloroform ($CDCl_3$) and deuterated methanol (CD_3OD), with chemical shifts referenced to tetramethylsilane (TMS). One-dimensional (1D) NMR experiments, including proton (^1H NMR), carbon (^13C NMR), and DEPT-135, were performed to determine the positions of hydrogen and carbon atoms and to identify structural fragments within the compound. In addition, two-dimensional (2D) NMR spectroscopy, specifically Heteronuclear Single Quantum Coherence (HSQC), was employed for precise assignment of proton and carbon chemical shifts.

The resulting spectra were processed and analyzed using MestroNova software to interpret the molecular structure of the compound.

2.4.3 LC-MS Analysis

Liquid Chromatography–Mass Spectrometry (LC-MS) was used to determine the molecular ion peak, base peak, and fragment (daughter) ions of the isolated compound PG1, providing insight into its molecular structure and mass.

3.0 Results and Discussion

3.1. Structural Characterization of PG1

The FTIR spectrum of PG1 reveals several key absorption bands that reflect its functional group composition, with comparisons drawn to reference peak values as shown in Table 1. A broad and intense peak at 3435.8 cm^{-1} corresponds to O–H stretching vibrations, which typically occur around 3400 cm^{-1}. The observed frequency is very close to the reference value, with a negligible deviation of +35.8 cm^{-1}, indicating the presence of hydroxyl groups engaged in hydrogen bonding.

Peaks at 2926.7 cm^{-1} and 2855.9 cm^{-1} are attributed to C–H stretching vibrations of aliphatic $–CH_2$ and $–CH_3$ groups. These peaks are comparable to standard reference values of 2925 and 2854 cm^{-1}, respectively. The minor deviations of +1.7 and +1.9 cm^{-1} suggest normal alkyl chain vibrations without significant structural strain or conjugative effects.

A sharp absorption at 1735.8 cm^{-1} is assigned to ester C=O stretching, which generally appears near 1740 cm^{-1}. The small deviation of –4.2 cm^{-1} implies a possible conjugation of the ester group with an adjacent aromatic ring, resulting in slight lowering of the vibrational energy.

The band at 1634.3 cm^{-1}, which is close to the standard aromatic or C=C stretching vibration near 1640 cm^{-1}, indicates the presence of conjugated alkenes or aromatic structures, with a deviation of –5.7 cm^{-1}. This could be due to extended conjugation or interaction with neighboring groups in the molecule.

Further analysis in the fingerprint region shows absorptions at 1457.4 and 1375.4 cm^{-1}, corresponding to CH_2 and CH_3 bending vibrations. These match well with their reference values of 1460 and 1375 cm^{-1}, with negligible deviations of –2.6 and 0.4 cm^{-1}, supporting the presence of saturated aliphatic chains.

The strong peak at 1235.3 cm^{-1}, slightly lower than the reference ester/ether C–O stretch at 1240 cm^{-1}, has a deviation of –4.7 cm^{-1}. This is indicative of C–O bonds in ester or ether linkages. Similarly, bands at 1166.8 cm^{-1}, 1107.2 cm^{-1}, and 1036.8 cm^{-1} (compared to reference values of 1170, 1110, and 1030 cm^{-1} respectively) exhibit minimal deviations (–3.2, –2.8, and +6.8 cm^{-1}), consistent with various C–O stretching vibrations found in alcohols and

glycosidic linkages. Lastly, the absorption at 873.5 cm^{-1} corresponds well with the reference value for aromatic para-substituted C–H out-of-plane bending at 870 cm^{-1}, with a deviation of only +3.5 cm^{-1}. This suggests a para-disubstituted aromatic ring in the structure of PG1. Overall, the IR spectral features of PG1 agree closely with reference peaks for hydroxyl, alkyl, ester, aromatic, and ether functional groups. The minimal deviations observed in Table 1 indicate that the compound has a stable conformation with no significant electronic perturbations. These results corroborate the structural assignments made from NMR data and support the presence of a polyfunctional molecule, such as a glycosylated phenolic ester.

Table 1: Comparison of FTIR Peak Positions of PG1 with Reference Frequencies and Deviations

Peak Position (cm^{-1})	Observed Functional Group	Reference Peak (cm^{-1})	Deviation (cm^{-1})	Additional Information
3435.8	O–H stretch (H-bonded)	3400	+35.8	Strong hydrogen bonding
2926.7	C–H asymmetric stretch (CH_2/CH_3)	2925	+1.7	Aliphatic chains
2855.9	C–H symmetric stretch (CH_2/CH_3)	2854	+1.9	Aliphatic chains
1735.8	C=O stretch (ester)	1740	–4.2	Slight conjugation with aromatic ring
1634.3	C=C stretch (aromatic/alkene)	1640	–5.7	Aromatic ring or conjugated alkene
1457.4	CH_2 bending	1460	–2.6	Saturated hydrocarbon
1375.4	CH_3 bending	1375	+0.4	Methyl group presence
1235.3	C–O stretch (ester/ether)	1240	–4.7	Ester or ether linkages
1166.8	C–O stretch (alcohol/ether)	1170	–3.2	Alcoholic or glycosidic oxygen
1107.2	C–O stretch	1110	–2.8	Alcohol/ether/glycosidic bonds
1036.8	C–O stretch	1030	+6.8	Alcohol or secondary ether
873.5	Aromatic C–H (para-substituted)	870	+3.5	Indicates para-substituted aromatic ring

The structural features of PG1 were further elucidated using both proton (^1H) and carbon (^{13}C) nuclear magnetic resonance (NMR) spectroscopy. These techniques provide detailed information on the types and environments of hydrogen and carbon atoms within the molecule. Table 2 presents the chemical shifts, types of protons and carbons, multiplicity, and number of protons associated with various positions in PG1.

The ^1H and ^{13}C NMR spectra further corroborate the structure proposed based on FTIR analysis. Aromatic protons resonate in the downfield region (6.45–7.78 ppm), which is consistent with substituted aromatic systems. Signals observed around 3.18–5.35 ppm are attributed to methine and methylene protons adjacent to oxygen, typical of alcohols and ethers.

The multiplicity of these peaks (triplet, doublet of doublets, etc.) provides insight into the coupling and neighboring hydrogen environments. The ^{13}C signals in the region of 100–156 ppm confirm the presence of aromatic and olefinic carbons, while the aliphatic carbon resonances are clearly visible in the 14–49 ppm range. Notably, the presence of multiple oxygen-bearing carbons (C–O) around 62–80

ppm confirms polyol-like structural features. These data align well with studies by Zhang *et al*. (2019), where similar chemical shifts were reported for glycosidic and phenolic compounds bearing multiple hydroxyl groups.

Table 2: ^{1}H NMR and ^{13}C NMR Data of PG1

Position	Chemical Shift (ppm)	Type of Carbon	Position	^{1}H Chemical Shift (ppm)	No. of Protons	Multiplicity
1	156.1	C=C	–	–	–	–
2	139.35	Ar–H	A	7.78	1H	s
3–4	130.2	C=C	–	–	–	–
5	129.94	Ar–H	H	7.44	1H	d
6	121.98	Ar–H	E	7.27	1H	d
7	76.89	CH–O	Q	3.52	1H	t
8	41.3	CH_2	C1	2.05	2H	dd
9	29.19	CH	Y	2.28	1H	td
10	26.43	CH	B1	2.18	1H	t
11–12	49.07	CH	A1	3.18	2H	td
...	...	...	...	...	...	...
29–30	17.55	Ar–CH_3	PI	2.40	6H	s
1'	100.04	CH–O	T	5.06	1H	d
2'–3'	62.37	CH–OH	M	5.35	1H	dd
–	–	OH	S	4.11	1H	s
4'	55.57	CH–OH	V	3.73	1H	m
–	–	OH	UI	4.61	1H	s
5'	80.10	CH–O	RI	4.25	1H	m
6'	61.30	CH_2–OH	O	4.50	2H	d
–	–	OH	P	5.16	1H	s

The presence of overlapping aromatic C=C stretches in the IR and corresponding downfield shifts in the ^{1}H and ^{13}C NMR spectra suggests a high degree of conjugation, likely due to substituted phenyl rings. The characteristic peaks of –CH_2OH, CH–OH, and CH–O groups are indicative of glycosylated or polyhydroxylated moieties, as found in many natural product derivatives such as flavonoid glycosides and saponins. In literature, Singh *et al*. (2017) observed ^{1}H signals around 4.5–5.5 ppm for proton environments in sugar derivatives, which corresponds to those observed at 5.06, 5.16, and 5.35 ppm in PG1. Additionally, Adeoye *et al*. (2022) highlighted strong IR bands near 3250 cm^{-1} for OH groups and 1600–1500 cm^{-1} for aromatic C=C, which are consistent with the present IR findings for PG1. The spectroscopic evidence from FTIR, ^{1}H NMR, and ^{13}C NMR collectively suggests that PG1 is a multifunctional compound featuring both aromatic rings and aliphatic chains, with multiple hydroxyl and ether linkages. This structural composition is in agreement with other polyhydroxylated aromatic compounds reported in natural product chemistry and supports the multifunctional behavior of PG1, potentially endowing it with interesting biological or material properties.

The proposed structure for PG 1, is a pentacyclic glycoside. It was eluted with a mixture of methanol and Pet. ether in the ratio of 90 : 10. The TLC (thin layer chromatography) experiment carried out on the sample gave a yellowish spot with an R_f value, 0.77. From the analysis of LC-MS (Liquid chromatography Mass Spectrometer), the compound exhibits a pseudo molecular ion peak at m/z = 624 with the molecular formular, $C_{41}H_{58}O_6$ (Schug, 2002; Pitt, 2009). The formation of the pseudo molecular ion / quasi molecular ion is as a result of the mode of ionization used which is ESI (electrospray ionization), that has the ability to protonate $[M + H]^+$, deprotonate $[M - H]^-$, forms

adduct ions which could be cationic or anionic, forms matrices and also, other cations like sodium and potassium, $[M + Na]^+$, $[M + K]^+$ could be added to it to enhance ionization and sensitivity. The spectrum also exhibited a base peak (peak with the highest intensity) at m/z = 313 and other fragment ions at m/z = 491, 488, 314, 181, 150, 120, etc.

Due to the poor resolution of Infrared spectrophotometer used for this analysis, prominent absorption bands could not be detected. However, overtones (harmonics) are observed at different regions and are represented in Table 1. These include: overtone at 3710.11 $cm^{-1,}$ which indicates the presence of moisture. Another overtone at 3253.73 cm^{-1}, which corresponds to O-H stretching vibration of an alcohol. There is also an overtone at 2919.20 cm^{-1}, which conforms to C-H stretching vibration of an aliphatic compound (Morrison and Boyd, 2005; Ugochukwu *et al*., 2020). Again, there are overtones at 1592.94 cm^{-1} and 1512.35 cm^{-1} which correspond to C=C stretching of aromatic rings. There is also an overtone at 1027.84 cm^{-1}, which corresponds to C-O stretching of alcohols and ethers.

^{13}C NMR (carbon - 13 Nuclear Magnetic Resonance) Spectrum tells how many different kinds of carbon a compound has. Another type of carbon -13 spectrum is DEPT-135 (Distortionless Enhancement by Polarization Transfer) Spectrum which is used to distinguish between CH_3, CH_2 and CH groups. DEPT -135 Spectrum shows CH_3 and CH in the positive x-axis while CH_2 is seen in the negative x-axis. The CH is seen downfield of the positive x-axis while CH_3 is seen upfield region (Bruice, 2011). Ordinary ^{13}C NMR Spectrum in conjunction with DEPT -135 Spectrum reveals different kinds of carbon which compound 1 (PG 1) has together with their chemical shift values (delta, δ - values in part per million, ppm) as represented in Table 2. This includes; methyl carbons (CH_3) which are represented in compound 1 as C-29 and C-30 at 17.55 ppm. These carbon atoms are bonded to aromatic rings and thereby experience deshielding by diamagnetic anisotropy (that is, the effect of pi bond). C-33 at δ 15.10 ppm is in an electron-dense environment. C-34 and C-35 at δ 14.42 ppm are in the same electron-dense environment. Another set of carbons is methylene carbon as revealed by DEPT -135 Spectrum, which are manually picked and are represented in the compound 1 as follows: C-8 at δ 41.30 ppm, it is somewhat deshielded because it is 2-J coupling to an electronegative atom, oxygen, which tends to draw electrons close to itself. C-13 and C-14 are in the same chemical environment and therefore, have the same frequency signal at δ 33.40 ppm. C-15 and C-16 at δ 21.30 ppm experience a shielding effect due to electron density, which causes them to resonate at a low frequency. C-21 and C-22 are also methylene carbon atoms,, which are in the same chemical environment and are shielded with a low resonance frequency signal at δ 35.01 ppm. Also, C-32 is a methylene carbon atom with a resonance frequency signal at δ 22.99 ppm. It is in an electron-dense environment and therefore, experiences shielding effect.

Again, C-6' (CH_2-OH) is also a methylene carbon atom with delta value at δ 85.42 ppm. It is highly deshielded by inductive effect as a result of an electron withdrawing group, hydroxy group (O-H) that is directly bonded to it and also, it is 2-J coupling to an oxygen atom in the sugar ring as well as another O-H group which is 3-bonds away. Another set of carbons as revealed by ^{13}C NMR/DEPT -135 Spectrum is methine carbons (CH) also known as tertiary carbon atoms and are represented in compound 1 as follows: C-7 (CH-O) at δ 76.89 ppm is an oxymethine carbon that is deshielded by inductive effect of an electronegative atom, oxygen that is directly bonded to it. C-10 at δ 26.43 ppm is in an electron dense environment. C-17 and C-18 are in the same chemical environment and therefore, have the same resonance frequency signal at δ 49.07 ppm. C-19 is also a methine carbon with chemical shift value at δ 32.58 ppm. C-20 is also a methine carbon with a low resonance frequency at δ 30.27 ppm.

C-1' (OCHO) is a dioxymethine carbon that is inductively deshielded with a very high resonance frequency signal at δ 100.02 ppm. It is an anomeric carbon atom which is bonded to two electronegative atoms (two oxygen atoms),

which tend to pull electrons close to themselves. There is also a Beta-glycosidic linkage between the anomeric carbon of the sugar moiety (glycon) and C-7 of the aglycone unit (non-sugar unit). C-2' (CH-OH) and C-3' (CH-OH) are hydroxymethine carbons which are in the same chemical environment with the same chemical shift value at δ 62.37 ppm. They experience deshielding by the inductive effect of an electron-withdrawing group, a hydroxy group which tends to pull electrons close to itself. C-4' (CH-OH) is also a hydroxymethine carbon which resonates inductively at δ 55.57 ppm. C-5' (CH-O) is an oxymethine with a high resonance frequency signal at 80.10 ppm. It is in an electron-poor environment because it is directly bonded to an oxygen atom in the sugar ring. Another part of the methine carbons are the aromatic carbons with proton attachments. This includes; C-2 (Ar-C) with a very high chemical shift value of δ 139.35 ppm is an aryl carbon that is highly deshielded by diamagnetic anisotropy of the aromatic ring. C-5 (Ar-C) at a high resonance frequency of δ 129.94 ppm is also an aryl carbon. C-6 (Ar-C) at δ 121.98 ppm, is also an aryl carbon which is in an electron-poor environment due to anisotropy.

C-24 (Ar-C) with a delta value of δ 119.47 ppm is an aryl carbon that experiences deshielding by anisotropy. C-25 (Ar-C) at δ 115.58 ppm is also an aryl carbon. C-26 (Ar-C) at δ 116.10 ppm is in an electron poor environment. Again, C-28 (Ar-C) at δ 111.18 ppm is an aryl carbon. Another set of carbons is quaternary carbons. These are carbons without hydrogen attachments. This includes; C-1 (C=C) at δ 156.10 ppm, an aromatic quaternary carbon that is highly deshielded. C-3 and C-4 (C=C) are aromatic quaternary carbons with the same chemical shift value of δ 130.20 ppm because, they are in the same chemical environment. C-23 (C=C) at δ 130.20 ppm is also an aromatic quaternary carbon. C-27 (C=C) at δ 156.10 ppm is an aromatic quaternary carbon. C-31 at δ 42.50 ppm is an aliphatic quaternary carbon. All these are represented in Table 2.

The number of signals in a ^{1}H NMR Spectrum tells how many different kinds of protons a compound has (Bruice, 2011). The structure of compound 1 contains hydrogens (protons) that are attached to various carbon atoms as revealed by the 1H NMR Spectrum of compound 1(PG 1), and are represented in the proposed structure as follows: five methyl protons which includes; H-29 (P1) (Ar-CH_3) which resonates at δ 2.40 ppm with a singlet (s) multiplicity. The three protons (3H) are bonded to a methyl carbon, which in turn is bonded to an aromatic ring. Therefore, the methyl proton experiences deshielding by diamagnetic anisotropy, and because there is no coupled protons (protons that are bonded to adjacent carbons), the signal cannot be split, and as such, the multiplicity is a singlet. H-30 is in the same chemical environment as H-29 and so, resonates at the same frequency with the same multiplicity. Again, H-33 (M1) resonates at δ 0.73 ppm with a doublet of doublets (dd). It is highly shielded because it is in an electron-dense environment. The multiplicity of doublet of doublets (dd) is so because the two protons bonded to the adjacent methylene carbon atom, which split the signal of methyl proton, are enantiotopic hydrogens bonded to a pro-chiral carbon. The two protons are chemically non-equivalent and so, the signals are split separately. Another methyl protons are H-34 and H-35 (O1) with a low resonance frequency at δ 14.42 ppm and a singlet (s) multiplicity.

Another set of protons as revealed by ^{1}H NMR Spectrum is methylene protons (CH_2). These protons are represented in the proposed structure of compound 1 as follows: H-32 (L1) at δ 0.85 ppm and a quartet (q) multiplicity. It is in an electron rich environment and thereby, resonates at a very low frequency. H-21 and H-22 (D1) are in the same chemical environment and therefore, resonate at the same frequency of δ 1.54 ppm with a multiplet (m). H-13 and H-14 (K1) are methylene protons in the same environment with a resonance frequency at 1.10 ppm and a quartet (q) multiplicity, they are in an electron rich environment.

H-15 and H-16 (N1) are methylene protons that are in the same environment and thereby, possess the same resonance frequency signal at δ 0.96 ppm and a quartet (q) multiplicity. The protons are highly shielded by electron density and therefore, they resonate at upfield region. H-8 (C1) resonates at δ 2.05 ppm and a doublet of

doublets (dd) multiplicity. The signal of this methylene proton is split separately by two non-equivalent adjacent methine protons. The methylene proton experiences deshielding because, the methylene carbon is bonded to an oxymethine carbon which withdraws electron inductively.

Also, H-6' (O) (CH_2-OH) is a hydroxy methylene proton that resonates with a very high resonance frequency at δ 4.50 ppm and a doublet (d) multiplicity. It is highly deshielded because it is directly bonded to an O-H group which draws electrons close to itself. Its O-H proton (P) resonates also at a very high frequency at δ 5.16 ppm with a singlet (s). The proton is deshielded because it is directly bonded to an oxygen atom that withdraws electrons. Another set of protons as revealed by ^{1}HNMR Spectrum is the methine protons (CH). This includes; H-7 (Q) (CH-O) is an oxymethine proton which resonates at δ 3.52 ppm with a triplet (t) multiplicity. The proton is inductively deshielded by its direct bond to an oxygen atom. H-9 (Y), which resonates at δ 2.28 ppm with a triplet of doublet (td) multiplicity, is a methine proton that is in an electron-dense environment.

Also, H-10 (B1) at δ 2.18 ppm with a triplet (t) multiplicity is a methine proton in an electron-dense environment. H-11, H-12, H-17 and H-18 (A1) are methine protons in the same chemical environment and resonate at the same frequency of δ 3.18 ppm with a triplet of doublet (td) multiplicity. Again, H-19 (N) at δ 2.86 ppm with a doublet (d) multiplicity is a methine proton in an electron-rich environment. H-20 (I1) which resonates at upfield region of δ 1.27 ppm with a multiplet (m) multiplicity, is also a methine proton in an electron-rich environment. Again, methine protons are present in the sugar region between δ 3.50 ppm to δ 5.50 ppm of the ^{1}H NMR Spectrum and are also represented in the proposed structure of compound 1 as; H-1' (T) (OCHO) at δ 5.06 ppm with a doublet (d) is a dioxymethine proton that is highly deshielded by inductive effect of the two oxygen atoms that are bonded to the methine carbon (which is the anomeric carbon of the sugar moiety).

H-2' and H-3' (M) (CH-OH) are hydroxymethine protons that are in the same environment and resonate inductively at a very high frequency of δ 5.35 ppm with a doublet of doublets (dd). Their hydroxy proton, O-H (S) also resonates at a high frequency of δ 4.11 ppm with a singlet (s) multiplicity. H-4' (V) (CH-OH) is also, a hydroxymethine proton that resonates inductively downfield at δ 3.73 ppm with a doublet of doublets (dd) multiplicity. Its hydroxy proton, O-H (U1) resonates inductively too at δ 4.61 ppm with a singlet (s) multiplicity. H-5' (R1) (CH-O) is an oxymethine proton which resonates at δ 4.50 ppm with a multiplet (m) multiplicity. The methine proton is deshielded downfield because it is directly bonded to an oxygen atom in the sugar ring and also, the methine carbon is bonded to a methylene carbon bearing an O-H group and a methine carbon bonded to another O-H group. Another part of the methine proton is the aromatic protons, which are represented thus: H-2 (A) (Ar-H) at a very high resonance frequency of δ 7.78 ppm with a singlet (s) multiplicity. This deshielding effect is caused by the diamagnetic anisotropy of the benzene ring. This assertion is supported by Bruice (2011).

H-5 (H) is another aryl proton with a high frequency signal at δ 7.44 ppm and a doublet (d) multiplicity, which is deshielded downfield by anisotropy. H-6 (Ar-H) is also an aryl proton which resonates at a high frequency of δ 7.27 ppm with a doublet (d) and it's deshielded downfield by anisotropy. H-24 (G) (Ar-H) at δ 6.84 ppm with a doublet (d) multiplicity is also an aryl proton that is deshielded by anisotropy. H-25 (K) (Ar-H) at δ 6.65 ppm and a doublet of doublets (dd) is a deshielded aryl proton. Again, H-26 (B) (Ar-H) with a high frequency signal at δ 6.74 ppm and a doublet (d) multiplicity is another aryl proton that is in an electron deficient environment due to anisotropy. Also, H-28 (L) at δ 6.45 ppm with a singlet (s) is an aryl proton which experiences deshielding downfield by anisotropy. All these are also represented in Table 4.8.

HSQC is an acronym for Heteronuclear Single Quantum Coherence. It is a 2- D NMR which involves an ^{1}H NMR on the x- axis and an ^{13}C NMR, DEPT- 135 to be precise, on the y-axis, determining proton - carbon single bond correlation between protons and their carbons, that is, which proton is bonded to which carbon.

The HSQC Spectrum of compound 1 (PG 1) reveals a correlation between C-33 (CH_3), a methyl carbon at δ 15.10 ppm and its proton (3H) at δ 0.73 ppm.

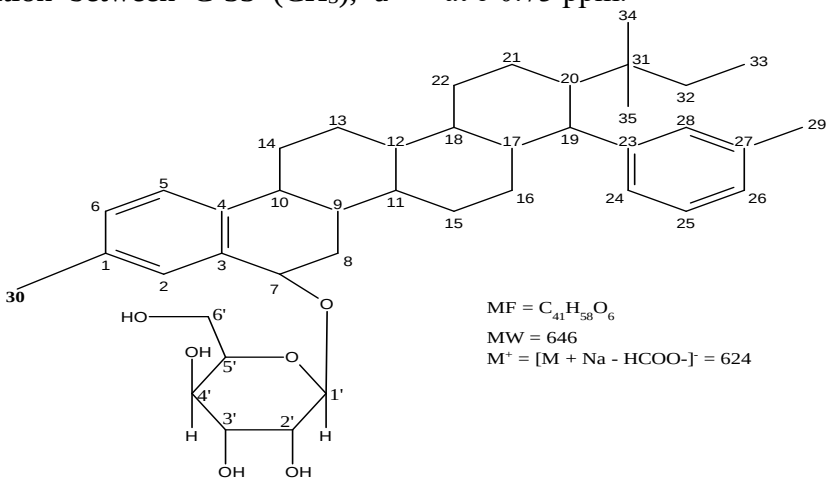

Fig 1: PG 1: (2*R*,3*R*,4*R*,5*R*,6*R*)-6'-(hydroxymethyl)-1-methyl-(20-(*tert*-pentyl)-19-(*m*-tolyl)-7,8,9,10,11,12,13,14,15,16,17,18,19,20,21,22-hexadecahydropicenyl) oxy)tetrahydro-2*H*-pyran-2,3,4-triol

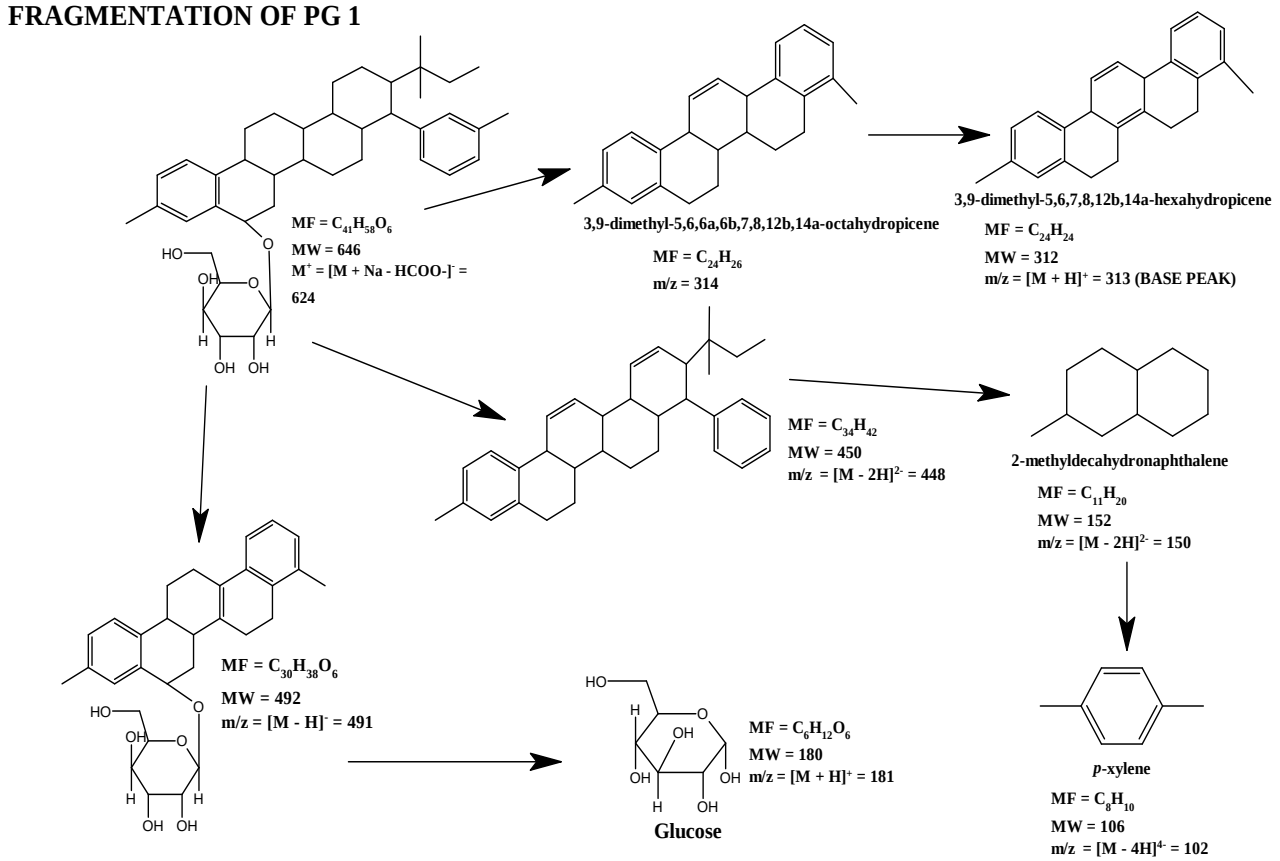

Fig 2: Fragmentation pattern of PG 1

There is a correlation between C-34 (CH_3) at δ 14.42 ppm and H-34 (3H) at δ 0.66 ppm with a singlet (s) multiplicity. There is also a correlation between a methine carbon, C-10 (CH) at δ 26.43 ppm and its proton (1H) at δ 2.18 ppm. There is also a correlation between C-20 (CH), a methine carbon at δ 30.27 ppm and its proton (1H) at δ 1.27 ppm. Another

correlation is between δ 40.19 ppm and δ 2.50 ppm which corresponds to DMSO (dimethyl sulfoxide) peak (solvent peak) and its protons respectively. Also, there is a correlation between C-11 (CH) at δ 49.07 ppm and its proton (1H) at δ 3.18 ppm. Again, there is a correlation between C-4' (CH-OH), a hydroxymethine carbon at δ 55.57 ppm and its proton (1H) at δ 3.73 ppm. Also, there is a correlation between C-5' (CH-O), an oxymethine carbon at δ 80.10 ppm and the proton that is bonded to it (1H), which resonates at δ 4.25 ppm.

Compound 1 (PG 1) is a derivative of oleanane, a natural pentacyclic triterpenoid. Oleananes and their derivatives constitute the most ubiquitous and important group of triterpenoids in the plant kingdom. They possess various pharmacological activities such as; anti-inflammatory activities as tested on albino rats. They also possess antiretroviral, antimalarial, anticancer and anti tumor activities (Holanda-Pinto *et al*., 2008).

4.0 Conclusion

The phytochemical investigation of *Allium sativum* stem bark led to the isolation of a bioactive compound from its ethyl acetate fraction, designated as PG1. Chromatographic purification followed by detailed spectral analysis—including ^1H and ^13C NMR, HSQC, FTIR, and mass spectrometry—enabled the elucidation of its structure. The compound was identified as a glycosylated oleanane-type pentacyclic triterpenoid. Similarly, chromatographic separation of the methanolic extract of air-dried purple garlic (*Allium sativum*) yielded a yellowish compound also coded as PG1, which was characterized as (2R,3R,4R,5R,6R)-6'-(hydroxymethyl)-1-methyl-(20-(tert-pentyl)-19-(m-tolyl)-7,8,9,10,11,12,13,14,15,16,17,18,19,20,21,22-hexadecahydropicenyl)oxy)tetrahydro-2H-pyran-2,3,4-triol. This compound shares structural features with the oleanane skeleton, a well-documented pharmacophore known for diverse biological activities.

The findings suggest that both *Allium sativum* is rich in glycosylated triterpenoids with significant medicinal potential. The successful structural identification of PG1 supports the ethnopharmacological relevance of these plants and provides a scientific basis for their traditional uses. In conclusion, PG1 is a promising candidate for further pharmacological evaluation due to its structural alignment with bioactive oleanane derivatives known for anti-inflammatory, antimalarial, and antitumor activities. It is recommended that further research be conducted to explore the pharmacodynamics, pharmacokinetics, and potential therapeutic applications of PG1, as well as to identify and characterize other bioactive constituents from these plant sources.

Acknowledgement

The authors are grateful to the Chemistry lab technologists, Michael Okpara University of Agriculture, Umudike, Abia State, Nigeria, for all the assistance rendered during the laboratory experiments of this work. Also, we are indebted to Mr. Chibuzor Olelewe of the University of Kentucky, USA, who ran all the spectral analyses without pay. The authors are equally grateful to Mr. Onyebuchi Ozoeze for funding this research work.

5.0 References

Block, E. (2010). Garlic and Other *Alliums*: The Lore and the Science. *Royal Society of Chemistry*, *9*78, pp. 190–199.

Mahady, G. B., Fong, H. H. S. & Farnsworth, N. R. (2001). *Botanical Dietary Supplements: Quality, Safety and Efficacy. Swets & Zeitlinger,* Lisse, The Netherland.

Hahn, G. (1996). *Garlic: The science and therapeutic application of Allium sativum L. and Related Species* (2nd ed). Baltimore Williams and Wilkins. pp. 1 - 24.

Newall, C. A., Anderson, L. A. & Phillipson, J. D. (1996). *Herbal Medicines: A Guide for Health Care Professionals*, London, England; *Pharmaceutical Press*, 9.p. 296.

Cavallito, C.J. and Bailey, J.H. (1944). Allicin, the antibacterial principle of Allium sativum. Isolation, physical properties and antibacterial action. *Journal of the American Chemical Society*, 66, pp. 1950–1951.

Orekhov, A. N. & Grunwald, J. (1997). Effects of garlic on atherosclerosis. *Nutrition*, 3, pp. 656–663.

JohnBull, E.O. & Afolabi, S.O. (2011). Bioactive evaluation of extracts of

Euphorbia hirta: The antimicrobial and anticholinesterase approach, *Journal of Phytomedicine and Therapeutics*, 6, 2, pp. 79-84.

Igwe, O.U. & Echeme, J.O. (2013). Isolation, characterization and antibacterial activity of 4-(4-phenyl-1,4-dihydronaphth alen-1-yl) pentenoic acid from the stem bark of *Brachystegia eurycoma* harms. *International Journal of Drug Development and Research*, 5, 2, pp. 335-340.

Kwekowe, C. G., Johnbull, E. O. & Otuokere, I. E. (2021). Isolation and characterization of secondary metabolite from the stem bark extract of *Allophylus africanus* Beauv (*Sapindaceae*). *Journal of Chemical Society of Nigeria*, 46, 2, pp. 0382 – 0392.

Schrader, B. (1995). *Infrared and raman spectroscopy: methods and applications*. New York: VCH, Weinheim. p. 787.

Schug, K.A. (2002). *Pseudo-Molecular Ion Formation by Aromatic Acids in Negative Ionization Mode Electrospray Ionization Mass Spectrometry.* Virginia Tech.

Pitt, J. J. (2009). *Principles and Applications of LC-MS in Clinical Biochemistry*. *Clinical Biochemistry Research*, 30, 1, pp. 19-34.

Morrison, R.T. & Boyd, R.N. (2005). *Organic chemistry*. 6th ed. Published by Asoke K. Ghosh, Prentice-Hall of India Pvt. Ltd., M-97, Connaught Circus, New Delhi. 585-642.

Ugochukwu, C. A., Okenwa, U.I., Friday, C. & Ibe - Diala, C. J. (2020). Isolation and Characterization of Stigmasterol and B-Sitosterol from the leaves of *Emilia coccinea* (Sims) G.Don. *Communication in Physical Science*, 6, 2, pp. 863-868.

Bruice, P.Y. (2011). *Organic Chemistry*. University of California, Santa Barbara. 6th ed. Prenticr Hall. Pp.501-622.

Holanda-Pinto, S. A., Pinto, L. M. S., Cunha, G. M. A., Chaves, M.H., Santos, F. A. & Rao, V. S. (2008). Anti-inflammatory effect of Amyrin, a pentacyclic triterpene from *Protium heptaphyllum* in rat model of acute periodontitis. *Inflammopharmacology*, 16, pp. 48-52.

Boonpeng, S., Siripongvutikorn, S., Sae-Wong, C. & Sutthirak, P. (2014). The antioxidant and anti-cadmium toxicity properties of garlic extracts. *Food Sciences and Nutrition*, 2, pp. 792–801.

Lee, D. Y., Li, H., Lim, H. J., Lee, H. J., Jeon, R. & Ryu, J. H. (2012). Anti-inflammatory activity of sulfur-containing compounds from garlic. *Journal of Medicinal Food*, 15, pp. 992–999.

Yun, H. M., Ban, J. O., Park, K.R., Lee, C. K., Jeong, H. S., Han, S. B. & Hong, J. T. (2014). Potential therapeutic effects of functionally active compounds isolated from garlic. *Pharmacology and Therapeutics*, 142, pp. 183–195.

Kimura, S., Tung, Y. C., Pan, M.H., Su, N.W., Lai, Y. J. & Cheng, K. C. (2017). Black garlic: A critical review of its production, bioactivity, and application. *Journal of Food and Drug Analysis*, 25, pp. 62–70.

Morihara, N., Hino, A., Miki, S., Takashima, M. & Suzuki, J. (2017). Aged garlic extract suppresses inflammation in apolipoprotein E-knockout mice. *Molecular Nutrition and Food Research*, 61, pp. 1700308, https://doi.org/10.1002/mnfr.201700308.

Declaration

Consent for publication

Not applicable

Availability of data

Data shall be made available on demand.

Competing interests

The authors declared no conflict of interest

Ethical Consideration

Not applicable

Funding

There is no source of external funding.

Authors' contributions

All the authors participated in all stages of the work under the supervision of JOE